THE JOURNAL OF BIOLOGICAL CHEMISTRY VOL. 288, NO. 28, pp. 20404–20415, July 12, 2013
© 2013 by The American Society for Biochemistry and Molecular Biology, Inc. Published in the U.S.A.

The Epac1 Signaling Pathway Regulates Cl^- Secretion via Modulation of Apical KCNN4c Channels in Diarrhea*

Received for publication, March 8, 2013, and in revised form, April 25, 2013 Published, JBC Papers in Press, May 17, 2013, DOI 10.1074/jbc.M113.467860

Irshad Ali Sheikh[‡1], **Hemanta Koley**[§], **Manoj K. Chakrabarti**[‡], **and Kazi Mirajul Hoque**[‡2]

From the Divisions of [‡]*Molecular Pathophysiology and* [§]*Microbiology, National Institute of Cholera and Enteric Diseases, P-33 CIT Road, Scheme-XM, Beliaghata, Kolkata 700010, India*

Background: Apical KCNN4c channel provides driving force for cAMP-induced Cl^- secretion.
Results: Epac1-Rap1A-RhoA-ROCK signaling affects Cl^- secretion via effects on the apical expression of KCNN4c channels.
Conclusion: This mechanism couples the surface expression of KCNN4c channels and Cl^- secretion in diarrhea.
Significance: Apical KCNN4c channels are a new target for adjunct therapy in diarrhea.

The apical membrane of intestinal epithelia expresses intermediate conductance K^+ channel (KCNN4), which provides the driving force for Cl^- secretion. However, its role in diarrhea and regulation by Epac1 is unknown. Previously we have established that Epac1 upon binding of cAMP activates a PKA-independent mechanism of Cl^- secretion via stimulation of Rap2-phospholipase Cϵ-$[Ca^{2+}]_i$ signaling. Here we report that Epac1 regulates surface expression of KCNN4c channel through its downstream Rap1A-RhoA-Rho-associated kinase (ROCK) signaling pathway for sustained Cl^- secretion. Depletion of Epac1 protein and apical addition of TRAM-34, a specific KCNN4 inhibitor, significantly abolished cAMP-stimulated Cl^- secretion and apical K^+ conductance ($I_{K(ap)}$) in T84WT cells. The current-voltage relationship of basolaterally permeabilized monolayers treated with Epac1 agonist 8-(4-chlorophenylthio)-2′-*O*- methyladenosine 3′,5′-cyclic monophosphate showed the presence of an inwardly rectifying and TRAM-34-sensitive K^+ channel in T84WT cells that was absent in Epac1KDT84 cells. Reconstructed confocal images in Epac1KDT84 cells revealed redistribution of KCNN4c proteins into subapical intracellular compartment, and a biotinylation assay showed ~83% lower surface expression of KCNN4c proteins compared with T84WT cells. Further investigation revealed that an Epac1 agonist activates Rap1 to facilitate $I_{K(ap)}$. Both RhoA inhibitor (GGTI298) and ROCK inhibitor (H1152) significantly reduced cAMP agonist-stimulated $I_{K(ap)}$, whereas the latter additionally reduced colocalization of KCNN4c with the apical membrane marker wheat germ agglutinin in T84WT cells. *In vivo* mouse ileal loop experiments showed reduced fluid accumulation by TRAM-34, GGTI298, or H1152 when injected together with cholera toxin into the loop. We conclude that Rap1A-dependent signaling of Epac1 involving RhoA-ROCK is an important regulator of intestinal fluid transport via modulation of apical KCNN4c channels, a finding with potential therapeutic value in diarrheal diseases.

Epithelial ion transport is a dynamic process that refers to both secretion and absorption of fluid and electrolytes across the gastrointestinal cells (1–4). Disturbances of this normal vectorial transport process under pathophysiologic conditions like pathogenic infection or genetic mutation often manifest diarrhea where either active secretion is enhanced, the absorption process is inhibited, or in some cases both are affected (5). In the case of secretory diarrhea, there is an enhanced Cl^- secretion along with Na^+ and water drawn osmotically into the intestinal lumen, leading to a massive loss of important electrolytes and fluid from the body and potentially death (6–10). For sustained loss of Cl^- through the apical Cl^- channels (CFTR[3] and calcium-activated chloride channel), not only must Cl^- be replenished through the basolateral NKCC1 co-transporter, but various K^+ channels must also maintain a favorable hyperpolarized condition to counteract Cl^- efflux-mediated depolarization of the cells. Thus, in epithelial function, second messenger-activated K^+ channels are essential players in the process of transepithelial Cl^- secretion (11). In gastrointestinal epithelial cells, they recycle K^+ across the membrane via multiple types of K^+ channels to maintain the driving force for Cl^- exit. A Ca^{2+}-activated K^+ channel(s) has been suggested to participate in the generation of the driving force for Cl^- secretion. Indeed, it is usually assumed that only a basolateral K^+ conductance produced from Ca^{2+} stimulation would actually facilitate the efficiency of the secretion mechanism (12, 13). However, there is considerable experimental evidence to suggest that the Ca^{2+}-activated K^+ channel of the intestinal apical membrane has a significant role in Cl^- secretion (14, 15). Although the Ca^{2+}-activated KCNN4 channel is expressed at

* This work was supported in part by Government of India, Ministry of Science and Technology, Department of Biotechnology Grant BT/HRD/35/02/07/2009 (to K. M. H.).

[1] Recipient of an Indian Council of Medical Research junior research fellowship.

[2] To whom correspondence should be addressed. Tel.: 91-801-722-6735; Fax: 91-33-2370-5066; E-mail: kmh_niced@yahoo.co.in.

[3] The abbreviations used are: CFTR, cystic fibrosis transmembrane conductance regulator; KCNN4, intermediate conductance calcium-activated K^+ channel 4; PLC, phospholipase C; ROCK, Rho-associated kinase; $I_{K(ap)}$, apical K^+ conductance; 8-pCPT-2′-*O*-Me-cAMP, 8-(4-chlorophenylthio)-2′-*O*-methyladenosine 3′,5′-cyclic monophosphate; WGA, wheat germ agglutinin; BK, large conductance calcium-activated potassium channel; Epac, exchange protein directly activated by cAMP; CT, cholera toxin; Isc, short circuit current; $I_{Cl(ap)}$, apical Cl^- conductance; I-V, current-voltage; FSK, forskolin; RalGDS-RBD, Ras-binding domain of the Ral guanine nucleotide dissociation stimulator; SK, small conductance calcium-activated potassium channel; CCH, carbachol; BAPTA-AM, 1,2-bis(2-aminophenoxy)-ethane-*N*,*N*,*N*′,*N*′-*tetraacetic acid tetrakis(acetoxymethyl ester);* DC-EBIO, 5,6-dichloro-1-ethyl-1,3-dihydro-2*H*-benzimidazole-2-one; I_{Cl}, Cl^- conductance; GTPγS, guanosine 5′-3-*O*-(thio)triphosphate.

both the apical and basolateral membranes in colonic epithelia, contribution of only the basolateral KCNN4 channel is credited for maintaining the favorable electrochemical gradient to sustain Cl^- secretion, thus neglecting the contribution of an apical KCNN4 channel (16). The significance of an apical K^+ channel was first highlighted by Cook and Young (17) in 1989 when they mathematically proved that apical K^+ channels actually increase Cl^- secretion in polarized secretory epithelia. Recently, Rajendran and co-workers (18) demonstrated that KCNN4c, the apical version of KCNN4 channel, provides the driving force for Cl^- secretion and contributes to stool K^+ loss during secretary diarrhea in rat distal colon.

KCNN4 is an intermediate conductance calcium-activated K^+ channel of the KCNN family and functions primarily in a variety of non-excitable cells including intestinal epithelia (19–21). Currently, three splice variants are known: KCNN4a, -b, and -c expressed in smooth muscle cells and the basolateral and apical membrane of colonic enterocytes, respectively (22). Although Ca^{2+} is the main modulator of the KCNN family of ion channels, cAMP has also been suggested to modulate these ion channels. This coupling or coordination between Ca^{2+} and cAMP has been most widely appreciated in the BK channel where cAMP and PKA-dependent phosphorylation shifts the affinity of the BK channels for Ca^{2+}, making it more active at physiological $[Ca^{2+}]_i$ (23). However, it has been demonstrated that BK channels play no essential role in the generation of the driving force for colonic electrogenic Cl^- secretion (24). An earlier study reported a dual mode of activation for the KCNN4 channel by these second messengers during physiological responses of the cells (25, 26). In line with these observations, we have demonstrated previously a link between two second messengers: cAMP and Ca^{2+} via exchange protein directly activated by cAMP (Epac1)-Rap2 signaling, which is involved in cholera toxin (CT)-stimulated Cl^- secretion. However, activation of Rap1 by cAMP is also achieved by the binding of cAMP to Epac proteins. The role of Rap1 in intestinal epithelial ion transport remains relatively unexplored. Epac activates Rap1 by catalyzing the conversion of GDP-Rap1 to GTP-Rap1, which is independent of classical cAMP/PKA signaling. Active GTP-Rap1 may act via its downstream RhoA-Rho-associated kinase (ROCK) pathway in the pathogenesis of secretory diarrhea.

Hence, the present study explored the hypothesis that Epac1 and its associated signaling may influence apical KCNN4c channel function via the Rap1-RhoA-ROCK signaling pathway in cAMP-stimulated Cl^- secretion. We used electrophysiology techniques that allow measurement of agonist-induced short circuit current (Isc) and apical K^+ conductance ($I_{K(ap)}$) in a polarized epithelium. The results indicate that activation of apical KCNN4c channels by Epac1 signaling is required to support Cl^- secretion induced by cAMP. Furthermore, our results strongly suggest that Epac1 and its downstream signaling might regulate the surface amount of functional KCNN4c protein. More importantly, the second key observation arising from our study is that potentially targeting the apical KCNN4c channel could provide a novel option to combat secretory diarrhea with oral rehydration solution therapy.

MATERIALS AND METHODS

Reagents

Unless otherwise stated, all chemicals used in this study were obtained from Sigma-Aldrich. Cell culture media and fetal bovine serum (FBS) were purchased from Cell Clone (catalogue number cc3021) and HiMedia (catalogue number RM9970), respectively. Puromycin (catalogue number ant pr-1) was purchased from InvivoGen. cDNA synthesis reagents were purchased from Invitrogen (catalogue number 11904-018), and Real Time PCR Master Mix was from Applied Biosystems (catalogue number 4309155). Penicillin-streptomycin was obtained from Invitrogen. Wheat germ agglutinin (WGA) was purchased from Molecular Probes. TRIzol (catalogue number 15596-026), FITC (catalogue number A11036), and Alexa Fluor 568-conjugated secondary antibody were from Invitrogen. C3 toxin (catalogue number CT04) was purchased from Cytoskeleton Inc. 8-pCPT-2′-*O*-Me-cAMP (catalogue number C051-01) was from Biolog Life Science Institute, Germany. KCNN4abc antibody was a gift from Dr. V. M. Rajendran's laboratory at the University of West Virginia, and GAPDH was obtained from Cell Signaling Technology.

Cell Culture

Wild type human colonic T84 intestinal epithelial cells (T84WT) and T84WT cells in which Epac1 is knocked down (Epac1KDT84 cells) were obtained from the Gastroenterology Division, The John Hopkins University. T84WT cells were routinely maintained in a 1:1 ratio of Dulbecco's modified Eagle's medium (DMEM) and Ham's F-12 medium supplemented with 10% fetal bovine serum, 100 units/ml penicillin, and 100 μg/ml streptomycin. For Epac1KDT84 cells, additional puromycin (10 μg/ml) was added in the media. Briefly, T84WT cells between passages 8 and 20 were seeded onto polycarbonate membrane, 12-mm Snapwell permeable support cell culture inserts (0.4-μm pore size; Costar, catalogue number 3407) and grown for 10–14 days during which time the media were changed every 48 h. Monolayer resistance was determined using an EVOM ohmmeter with STX2 electrodes (World Precision Instruments, Inc.). Monolayers were considered polarized and mounted in an Ussing chamber when resistance was equal to or greater than 1,500 ohms/cm^2.

RNA Interference

Rap1A and Rap1B Knockdown by Lenti-shRNA—The RNA Interference Consortium (TRC) lentivirus-based short hairpin RNAs (shRNAs) were used to knock down Rap1A and Rap1B in T84WT cells according to our previously described method (27). In brief, gene sequence-specific shRNA clones constructed within the lentivirus plasmid vector pLKO.1-puromycin were obtained from Sigma-Aldrich. Four lentivirus-mediated shRNAs for each gene were designed to trigger the gene silencing (shown in Table 1). Stable cell lines of T84WT with expression of Rap1A and Rap1B knocked down were generated by infecting cells with respective gene-specific lenti-shRNA particles, and positively transduced cells were selected with 10 μg/ml puromycin-containing medium. mRNA expression in transduced cells was evaluated by quantitative PCR as well as by

TABLE 1
Lenti-shRNA constructs used for gene silencing in this study

Protein	Construct
Rap1a	1-TRC29784
	2-TRC29785
	3-TRC29786
	4-TRC29787
Rap1b	1-TRC29174
	2-TRC29175
	3-TRC29177
	4-TRC29178

measuring Isc. The lenti-shRNA construct specific for green fluorescence protein (GFP) was transduced in T84WT cells and served as a negative control. The efficiency of lentivirus-mediated siRNA infection in T84WT cells was determined using fluorescence microscopy to observe lentivirus-mediated GFP expression (data not shown).

Real time PCR (Quantitative PCR)—Analysis of mRNA expression was performed and compared with GAPDH using the difference of PCR cycles to reach a threshold amplification (ΔC_T), and the relative amount of the target mRNA is given as $2^{-(\Delta CT)}$. Real time PCR was performed on an Applied Biosystems AB7900 real time PCR detection system programmed as follows: step 1, one cycle, 50 °C for 2 min; step 2, one cycle, 95 °C for 10 min; step 3, 45 cycles, 95 °C for 15 s, 60 °C for 30 s, and 72 °C for 30 s; step 4 (dissociation; ramp rate, 2%), 95 °C for 15 s, 60 °C for 15 s, and 95 °C for 15 s. Amplification reactions were performed in a final volume of 25 μl containing cDNA from 30 ng of reverse transcribed total RNA, 300 nM each of forward and reverse primers for Rap1A (forward, GACCTGAGGGAACAGATTTTAC; reverse, CCTGCTCTTTGCCAACTAC; NCBI RefSeq accession number NM_001010935) and Rap1B (forward, TTCCATCACAGCACAGTCC; reverse, CCCTACAACTCTTTCATCTTCC; NCBI RefSeq accession number NM_001010942.1), and SYBR Green PCR Master Mix. The forward and reverse primers for GAPDH were GTCTCCTCTGACTTCAACA and CAGGAAATGAGCTTGACAAA, respectively. To control for specific PCR products, a dissociation curve was generated after the end of the last cycle.

Electrophysiology

Measurement of Transepithelial Isc—T84WT and Epac1KDT84 cells grown on Snapwell inserts were mounted in an Ussing chamber, and transepithelial potential differences were clamped to 0 mV using a VCC MC6 multichannel voltage-current clamp amplifier (Physiologic Instruments) as described previously (11). The Isc was continuously recorded using Ag-AgCl electrodes in 3 M KCl agar bridges. Apical and basolateral solutions were maintained at 37 °C by heated water jackets and separately perfused and oxygenated with 100% O_2. The bath Ringer's solution contained 140 mM NaCl, 5 mM KCl, 1 mM $MgCl_2$, 2 mM $CaCl_2$, 10 mM glucose, and 10 mM HEPES adjusted to pH 7.4. The change in Isc induced by the treatment was expressed as the difference from the base line to the steady state.

Measurement of Apical Potassium and Chloride Current—$I_{K(ap)}$ was assessed by applying a high basolateral to low apical $[K^+]$ gradient across the monolayers followed by permeabilization with the monovalent ionophore nystatin used previously (27, 28). After mounting Snapwell inserts in an Ussing chamber, normal Ringer's solution in the apical hemichamber was replaced with low K^+ buffer solution containing 137 mM *N*-methyl-D-glutamate, 5 mM potassium gluconate, 0.4 mM $MgSO_4$, 1.25 mM $CaCl_2$, 0.43 mM KH_2PO_4, 0.35 mM K_2HPO_4, 10 mM glucose, and 10 mM HEPES, and in the basolateral chamber, it was replaced with high K^+ buffer solution containing 143 mM potassium gluconate, 0.4 mM $MgSO_4$, 1.25 mM $CaCl_2$, 0.43 mM KH_2PO_4, 0.35 mM K_2HPO_4, 10 mM glucose, and 10 mM HEPES.

Apical Cl^- conductance ($I_{Cl(ap)}$) was assessed after permeabilization of the basolateral membrane with 50 μg/ml nystatin and the establishment of a basolateral to apical Cl^- concentration gradient as described previously (27). For the measurement of $I_{Cl(ap)}$ current, we did not use the customary Ussing convention for Iscs where the voltage is V2-V1 where V1 represents basolateral and V2 represents apical (apical-basolateral) voltage. Instead, we used the physiological convention of inside-outside, which when the basolateral side has been permeabilized to Cl^- can also be thought of as basolateral-apical. In the measurement of $I_{K(ap)}$, we kept the "Ussing convention" of apical-basolateral. The switching of conventions results in switching polarity but nothing else and allows for a comparison of the properties of the channels described here with those of others (27).

Current-Voltage (I-V) Relationship Study—To study the K^+ conductance of apical plasma membrane for the generation of an I-V relationship, the voltage across the monolayer was sequentially stepped from a holding voltage of 0 mV to values between −100 and +100 mV in 20-mV increments with a pulse duration of 5 s, and corresponding currents were recorded. A 50-s interval between each pulse was sufficient for recovery from activation. The protocol was performed after sustained stimulation with forskolin or 8-pCPT-2′-*O*-Me-cAMP. I-V plots of current recordings of nystatin-permeabilized T84WT cells were performed under a symmetrical (basal/apical) K^+ gradient (143 mM).

Western Blot

T84WT and Epac1KDT84 cells grown to confluence on a Transwell permeable support (75-mm diameter; Costar, catalogue number 3419) were washed and scraped in PBS solution and then homogenized by sonication in radioimmune precipitation assay buffer with protease inhibitor mixture (1:100; Sigma) to obtain cell lysate. Total cell lysate from different region of mouse intestine were prepared as reported previously (29). These cell lysates were separated by 10% SDS-PAGE and blotted to nitrocellulose membrane. These membranes were blocked with 5% nonfat dried milk for 1 h at room temperature and incubated overnight with primary antibody at 4 °C. The primary antibodies used were anti-KCNN4abc antibody (dilution, 1:3,000) and anti-GAPDH antibody (dilution, 1:5,000). The KCNN4abc antibody we used also detects both KCNN4b and KCNN4c as documented by a previous study (22). IRDye 800- or 680-conjugated anti-mouse or anti-rabbit IgG (1:15,000; Rockland Immunochemicals, Gilbertsville, PA) was used as a secondary antibody for 1 h followed by three washes. The fluorescence signal was analyzed using the Odyssey infra-

red system at 700- and 800-nm wavelengths (LI-COR Biosciences) as described previously (27).

Surface Biotinylation

Cell monolayers were grown on 6-well (top three inserts for T84WT and bottom three inserts for Epac1KDT84 cells) Transwell inserts (Costar, catalogue number 3450) for detection of total and surface amounts of KCNN4c and KCNN4b by surface biotinylation as described earlier (30, 31). Briefly, cells grown on Transwell inserts were serum-starved for 4 h followed by rinsing three times with ice-cold phosphate-buffered saline (150 mM NaCl and 20 mM Na_2HPO_4, pH 7.4) and once in borate buffer (154 mM NaCl, 1.0 mM boric acid, 7.2 mM KCl, and 1.8 mM $CaCl_2$, pH 9.0). Cells (both surfaces) were then incubated for 20 min with 0.5 mg/ml NHS-SS-biotin (succinimidyl 2-(biotinamido)-ethyl-1,3′-dithiopropionate biotinylation solution; Pierce), and this was repeated once. Cells were then washed three times with the quenching buffer (20 mM Tris and 120 mM NaCl, pH 7.4) to scavenge the unbound NHS-SS-biotin. Monolayers were washed with ice-cold PBS and scraped off their filter support in N^+ buffer (60 mM HEPES, pH 7.4, 150 mM NaCl, 3 mM KCl, 5 mM Na3EDTA, 3 mM EGTA, and 1% Triton X-100). The lysate was agitated for 30 min and spun at 14,000 × *g* for 15 min to remove the insoluble cell debris. An aliquot was retained as the total cellular KCNN4 protein. Protein concentration was determined, and 1 mg of lysate was then incubated with streptavidin-agarose beads overnight. The streptavidin-agarose beads were washed five times in N^+ buffer to remove nonspecifically bound proteins. All the above procedures were performed at 4 °C or in ice. Biotinylated surface proteins were then solubilized in an equivalent volume of sample buffer (5 mM Tris-HCl, pH 6.8, 1% SDS, 10% glycerol, and 1% 2-mercaptoethanol) and boiled for 5 min. Dilutions of the total and surface KCNN4c and KCNN4b were resolved by 10% SDS-PAGE and immunoblotted with anti-KCNN4abc antibody. Western analysis and quantification of the surface fraction were performed using the Odyssey system and Odyssey software (LI-COR Biosciences) as described under "Materials and Methods." Multiple volumes for each total and surface sample were used with linear regression with intensity of signal to obtain a single value for each sample. The percentage of surface KCNN4c was calculated from the ratio ((surface KCNN4c signal/total KCNN4c signal)) × dilution factor of surface and total KCNN4c samples and expressed as the percentage of total KCNN4c.

Immunofluorescence Study

Transwell insert-grown T84WT cell monolayers were fixed on ice in 3% paraformaldehyde solution (catalogue number 15710; Electron Microscopy Sciences, Hartfield, PA) in PBS, pH 7.4 at 4 °C for 20 min. Monolayers were then washed in ice-cold PBS, quenched with 50 mM NH_4Cl in PBS for 15 min on ice, and excised as circles from the inserts. The fixed cell monolayers were then permeabilized for 30 min in 0.1% saponin in PBS before being blocked for 30 min in PBS + 1% BSA supplemented with 10% FBS. Cell monolayers were incubated with primary antibody in PBS + 1% BSA for 1 h at room temperature in a moist environment. After three 10-min washes in PBS + 0.1% saponin, monolayers were incubated with Alexa Fluor 568-conjugated goat secondary antibody diluted 1:100 in PBS + 1% BSA for 1 h at room temperature in a moist and dark environment. Inserts were then rinsed four times for 10 min in PBS + 0.1% saponin, cut into rectangles, placed on glass slides, mounted in mounting medium (Sigma), and examined on a Zeiss LSM 510 laser-scanning confocal fluorescence microscope (×63 objective, oil immersion). To label the apical surface of T84WT cells, confluent cell monolayers were labeled with 1 μg/ml FITC-conjugated WGA prior to permeabilization and staining for KCNN4c channel. For staining of mouse intestinal tissue sections, the intestine was dissected, and the colon was rinsed with ice-cold saline and fixed in 3% paraformaldehyde prior to standard paraffin embedding as described (32, 33). Briefly, individual sections were heat-fixed and deparaffinized followed by microwave treatment in 0.01 M sodium citrate solution for antigen recovery. Endogenous peroxidase activity was blocked by a 30-min preincubation in H_2O_2 (Sigma). Sections were then washed in PBS and blocked with 5% normal goat serum (Sigma) in PBS for 30 min at room temperature. Subsequently, sections were incubated with primary antibody diluted in 5% normal goat serum in PBS for 1 h at room temperature followed by FITC-conjugated goat secondary antibody, and images were obtained using a Zeiss LSM 510/META confocal microscope.

In Vitro Activation of Rap1

Activation of Rap1 was determined by the EZ-Detect Rap activation kit (Pierce, catalog number 89872) as described previously with slight modification (27). Serum-deprived cells were stimulated with or without forskolin (FSK) and 8-pCPT-2′-*O*-Me-cAMP for 20 min at 37 °C and then lysed in lysis buffer (provided in the kit) in the presence of protease inhibitor mixture. After lysis, samples were centrifuged at 14,000 × *g* at 4 °C for 10 min, and the protein concentrations of the lysates were measured. 500 μg of cell lysates were immediately affinity-precipitated at 4 °C for 1 h with 20 μg of glutathione *S*-transferase-tagged Ras-binding domain of the Ral guanine nucleotide dissociation stimulator (RalGDS-RBD) following the manufacturer's protocol. Activated Rap1 (Rap1-GTP) was eluted in 50 μl of Laemmli sample buffer and detected by Western blotting using an antibody specific to Rap1.

Mouse Ileal Loop Experiment

The ileal loop experiment was performed in 6–8-week-old mice by a modified rabbit ileal loop assay originally described by De and Chatterje (34). Prior approval for the animal experiment was obtained from the Institutional Animal Ethics Committee (approval number Apro/75/24/11/2010, November 24, 2010). Following gut sterilization, the animals were kept fasted for 24 h prior to surgery and fed only water *ad libitum*. Anesthesia was induced by a mixture of ketamine (35 mg/kg of body weight) and xylazine (5 mg/kg of body weight). A laparotomy was performed, and the experimental loops of 5-cm length were constricted at the terminal ileum by tying with non-absorbable silk. The following fluids were instilled in each loop by means of a tuberculin syringe fitted with a disposable needle through the ligated end of the loop as the ligatured was tightened: pure CT (1 μg; positive control), saline (negative control), CT (1 μg) +

TRAM-34 (different concentrations in μM as indicated in Fig. 7), CT (1 μg) + H1152 (1 μM), and CT (1 μg) + GGTI298 (different concentrations in μM), a specific inhibitor of Rap1A. The intestine was returned to the peritoneum, and the mice were sutured and returned to their cages. After 6 h, these animals were sacrificed by cervical dislocation, and the loops were excised. The fluid from each loop was collected, and the ratio of the amount of fluid contained in the loop with respect to the length of the loop (fluid accumulation ratio in g/cm) was calculated as a reflection of the efficacy of various inhibitors.

Statistical Analysis

Results are expressed as means ± S.E. Paired and unpaired *t* tests were used to compare mean values within one experimental series. $p < 0.05$ was accepted to indicate statistical significance.

RESULTS

KCNN4 Channel Blocker Inhibits cAMP-stimulated Cl^- Secretion in Intestinal Epithelial Cells—To directly test the hypothesis that apical K^+ channels play a role in providing the driving force for the cAMP-stimulated Cl^- secretion, we first investigated the pharmacological profile of various K^+ channel blockers added on the apical side after the adenylate cyclase activator FSK stimulated Isc, a measure of Cl^- secretion. FSK elicits Cl^- secretion in T84WT cells via elevation of cAMP and activation of protein kinase A and Epac1 (27, 35). Fig. 1*A* shows the inhibitory effect in Isc responses of FSK to the effective concentrations of various K^+ channel blockers. We found that clotrimazole (91 ± 4% of control), which is often used as a probe of Ca^{2+}-activated K^+ channels (36, 37), and TRAM-34 (97 ± 3% of control), a specific Ca^{2+}-activated KCNN4 channel blocker, almost completely inhibited Cl^- secretion stimulated by FSK. However, addition of apamin, a specific SK channel blocker; iberiotoxin, a specific BK channel blocker; tetraethylammonium, a nonspecific K^+ channel blocker; and $ZnCl_2$, a KCNQ1/KCNE3 channel blocker, had no effect on FSK-stimulated Isc. $BaCl_2$, a nonspecific K^+ channel blocker, only required a 5 mM concentration to significantly (21 ± 4 *versus* 32 ± 2 μA/cm^2 (34%), $p < 0.05$) reduce FSK-stimulated Isc. The complete inhibition by lipophilic clotrimazole and TRAM-34 represents both apical and basolateral KCNN4 channels, whereas the inhibitory effect of impermeable $BaCl_2$ in intact cells or apical TRAM-34 in basolaterally permeabilized T84 cells represents only inhibition of apical KCNN4 channels. Zinc had a biphasic effect on KCNQ1/KCNE3 in T84WT cells (38) and was used to establish that KCNQ1/KCNE3 is not on the apical membrane. This is critical because basolateral membrane K^+ channels composed of KCNQ1 and the KCNE3 ancillary subunit play a critical role in epithelial tissue Cl^- secretion by establishing electrical driving force. The complete inhibition of FSK-stimulated Isc by clotrimazole and TRAM-34 compared with the lack of effect of apamin, iberiotoxin, or zinc suggests a possible role for apical KCNN4 channels but not BK, SK, or KCNQ1/KCNE3 channels in cAMP-stimulated Cl^- secretion.

To further show that TRAM-34 inhibits FSK-stimulated Cl^- secretion via blockage of the apical KCNN4 channel, we examined $I_{K(ap)}$ by applying a basolateral to apical K^+ gradient with

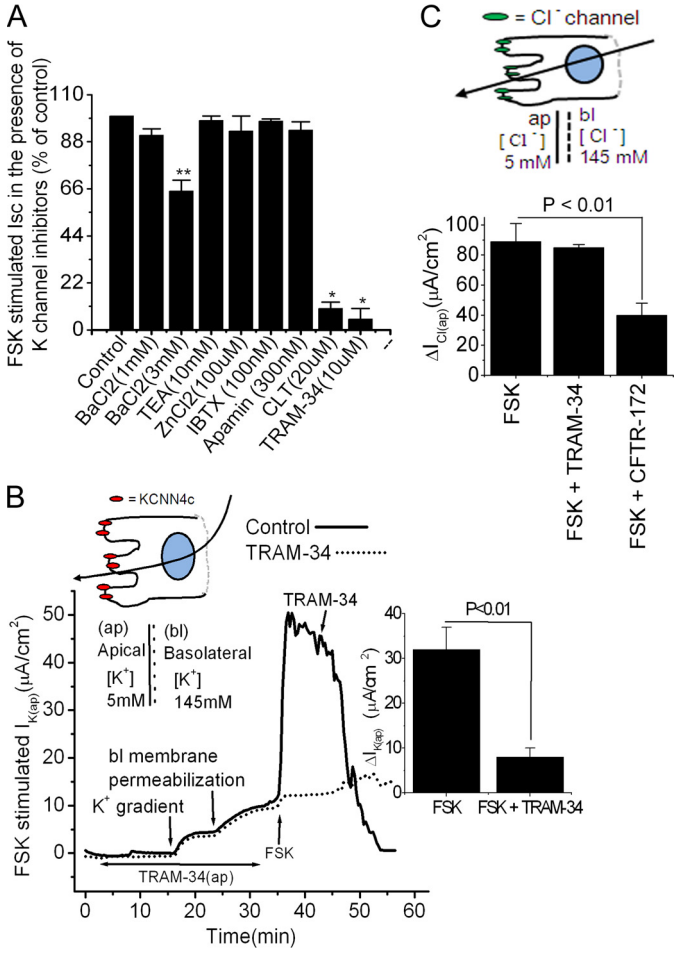

FIGURE 1. **Effect of K^+ channel blockers on FSK-stimulated currents of the human intestinal T84WT cell monolayers grown on Transwell insert.** *A*, summary of calculated Isc in the presence of various K^+ channel blockers in intact T84WT cells. FSK-stimulated Isc in the absence of K^+ channel inhibitor was set to 100% (control). *B*, representative trace of the effect of apical TRAM-34 (10 μM) on $I_{K(ap)}$ of T84WT monolayer with basolaterally permeabilized membrane. $I_{K(ap)}$ was measured as described under "Materials and Methods." TRAM-34 was applied either apically before 30 min of FSK stimulation or after as indicated. The *inset* shows the summary of the mean effect of TRAM-34 on $I_{K(ap)}$ from three independent experiments. The single cell illustration (*top*) indicates the direction of the K^+ gradient, and the *dashed line* indicates the permeabilization of the basolateral membrane with nystatin. *C*, summary of the data from six monolayers of T84WT cells permeabilized by basolateral nystatin as described previously (28) showing that TRAM-34 did not have any inhibitory effect on FSK-stimulated $I_{Cl(ap)}$ (10 μM FSK was added to the basolateral membrane). The illustration of the cell (*top*) indicates the direction of the Cl^- gradient, and the *dashed line* indicates the permeabilization of the basolateral membrane with nystatin. $\Delta I_{K(ap)}$ or $\Delta I_{Cl(ap)}$ was derived from values before and after FSK stimulation. Values are mean ± S.E. *Asterisks* indicates significant difference: *, $p < 0.001$ and **, $p < 0.05$ when compared with control; $n = 6–10$. *Error bars* represent S.E. *bl*, basolateral; *IBTX*, iberiotoxin; *CLT*, clotrimazole; *TEA*, tetraethylammonium; *ap*, apical.

K^+ as the sole permeant ion as described under "Materials and Methods" (39). After nystatin permeabilization of the basolateral membrane and in the presence of this K^+ gradient, FSK elicited a rise in $I_{K(ap)}$ that was significantly (32 ± 5 *versus* 8 ± 2 μA/cm^2, $p < 0.01$) inhibited by 10 μM TRAM-34 (Fig. 1*B*), and TRAM-34 did not have any effect on $I_{Cl(ap)}$ measured after permeabilization of the basolateral membrane and the establishment of a basolateral to apical Cl^- conductance gradient as described previously (27). In contrast, the addition of the CFTR inhibitor $CFTR_{inh}$-172 to the apical membrane led to a marked

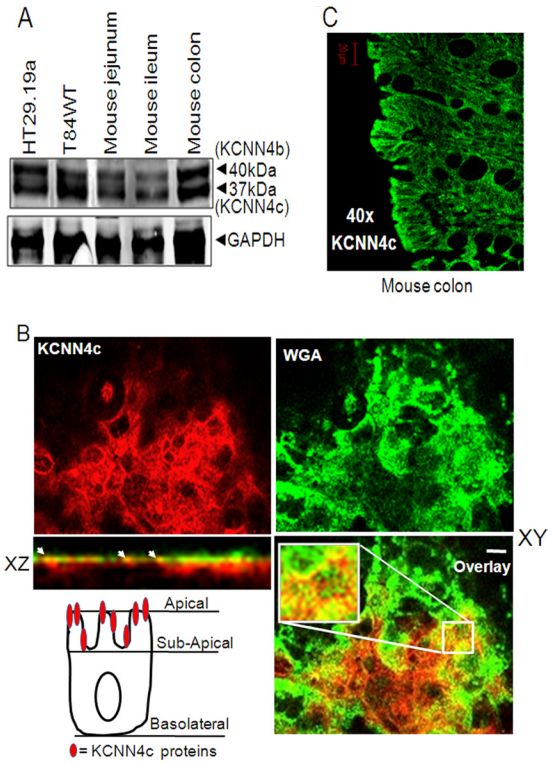

FIGURE 2. **Expression and polarization of KCNN4c on the apical membrane of intestinal epithelial cells and mouse intestine.** *A*, proteins from total lysate of mouse intestinal tissues and human colonic cell lines were resolved by 10% SDS-PAGE as described under "Materials and Methods" and immunoblotted with KCNN4abc antibody. KCNN4 proteins migrate in all cases as two major bands with apparent molecular masses of 37 (KCNN4c) and 40 kDa (KCNN4b), respectively. *B*, colocalization of KCNN4c (*red*) with the apical membrane marker WGA (*green*) in T84WT cells. Polarized T84WT cells were grown on Transwell inserts and analyzed in *xy* and *xz* scans by confocal microscopy as described under "Materials and Methods." The *xy* confocal section of T84WT cells shows clear apical membrane staining of KCNN4c colocalized with WGA. Colocalization is reflected by a *yellow* signal of the merged composite of *xy* and *xz* sections (*bottom*); the culture surface is at the *bottom* of image, and the apical surface of the cells is at the *top*. The merged image is shown in the *bottom panel*. *Insets* show enlarged regions within the *white box*. The *xz* plane of the region marked in the *white square* is shown at the *bottom*. *Scale bars* represent 10 μm. The cell illustration (*bottom left*) indicates the presence of functional KCNN4c on the apical most membrane but not beneath the subapical membrane in T84WT cells. *C*, KCNN4c in mouse colon. Paraffin sections of mouse colonic tissues were fixed and stained for KCNN4c (*green*), and *xy* images were collected by confocal microscopy as described under "Materials and Methods." *White arrows* indicate colocalization hot spots.

inhibition of $I_{Cl(ap)}$ (Fig. 1*C*). All these data when taken together suggest that apical KCNN4 channels may be required for cAMP-stimulated transepithelial Cl^- secretion.

Detection of Apical Expression of KCNN4 Channels by Western Blot and Confocal Microscopy in T84WT Cells and Mouse Intestinal Epithelia—To examine KCNN4 protein expression in different parts of mouse intestine and different intestinal epithelial cell lines, Western blot analysis was performed using a KCNN4abc antibody. Previous studies (22, 40) have shown that two isoforms, KCNN4c and KCNN4b, localize to the apical and basolateral membranes, respectively, in rat colon. We hoped to determine whether they are also present in human intestinal carcinoma cell lines and in mouse intestine. Fig. 2*A* shows a strong KCNN4c immunoreactive signal in different regions of mouse intestine as well as in T84WT and HT29.19a cells. KCNN4 protein migrates as two major bands in all cases with apparent molecular masses of 37 and 40 kDa. This finding confirms the expression of the apical (37-kDa) and basolateral (40-kDa) versions of KCNN4 channel termed KCNN4c and KCNN4b, respectively, in epithelial cell homogenates as reported previously (40). To confirm apical expression of KCNN4 in mouse colon and in T84WT cells grown in Transwell inserts, a confocal study using a KCNN4abc antibody was carried out. The *xy* and *xz* images of T84WT cells shown in Fig. 2*B* confirmed apical expression of KCNN4 channel by its colocalization with the apical surface marker WGA, which binds specifically to sugar residues expressed on the apical membrane of the cell. We further confirmed apical expression of KCNN4 in the mouse colon by immunostaining as shown in Fig. 2*C*.

Epac1 Influenced $I_{K(ap)}$ by Regulating Apical KCNN4 Channel in T84WT Cells—Our previous study identified an additional cAMP signaling pathway that activates PKA-independent, Epac1-mediated intestinal Cl^- secretion through a non-CFTR Cl^- channel (27). Epac1 increases $[Ca^{2+}]_i$ through activation of Epac1-Rap2-PLCϵ-Ca^{2+} signaling cascades (27). Because KCNN4 channels are regulated by $[Ca^{2+}]_i$, we next investigated the role of Epac1, if any, in $I_{K(ap)}$ using nystatin-permeabilized T84WT cells. In the presence of an apically directed K^+ gradient, addition of FSK failed to raise $I_{K(ap)}$ in Epac1KDT84 cells; this was significantly different from T84WT cells (5 ± 0.8 *versus* 32.3 ± 2.7 $\mu A/cm^2$, $p < 0.005$; Fig. 3*A*). Unexpectedly, serosal application of the $[Ca^{2+}]_i$-elevating agent carbachol (CCH) in Epac1KDT84 cells also resulted in a significant reduction of $I_{K(ap)}$ when compared with T84WT cells (20 ± 5 *versus* 69 ± 4 $\mu A/cm^2$, $p < 0.01$; Fig. 3*B*). These data of $I_{K(ap)}$ in Epac1KDT84 cells compared with those in T84WT cells in response to FSK and CCH indicate that Epac1 is required for the agonist-stimulated Cl^- secretion, which influences the $I_{K(ap)}$. Next we sought to ascertain whether apical KCNN4c contributes to the $I_{K(ap)}$ observed in the previous experiments. We studied the I-V relationships in basolaterally permeabilized monolayers of T84WT and Epac1KDT84 cells treated with the Epac1 agonist 8-pCPT-2′-*O*-Me-cAMP or in the presence of TRAM-34 in a symmetric K^+ ion concentration. Fig. 3*C* demonstrates the presence of a moderately inwardly rectified K^+ channel in T84WT cells that was activated by 8-pCPT-2′-*O*-Me-cAMP and blocked by TRAM-34. Interestingly, 8-pCPT-2′-*O*-Me-cAMP was not able to activate this inwardly rectifying current in Epac1KDT84 cells. Furthermore, with the symmetric K^+ ion concentration, the I-V curve became more or less linear when a voltage ramp (-60 to $+60$ mV) was applied. We also determined the calcium dependence of 8-pCPT-2′-*O*-Me-cAMP-stimulated $I_{K(ap)}$ current in T84WT cells in the presence or absence of the $[Ca^{2+}]_i$ chelator BAPTA-AM. As shown in Fig. 3*C*, *inset*, treatment with 8-pCPT-2′-*O*-Me-cAMP increased $I_{K(ap)}$, which was significantly inhibited by BAPTA-AM. Furthermore, addition of the KCNN4 channel-specific activator DC-EBIO at the apical side of intact T84WT cells resulted in a 44 ± 5 $\mu A/cm^2$ rise in Isc. In contrast, DC-EBIO enhanced Isc only 5 ± 1 and 4 ± 3 $\mu A/cm^2$ in Epac1KDT84 cells and T84WT cells treated with TRAM-34 (10 μM), respectively (Fig. 3*D*). Together these data indicate that Epac1 may influence an inwardly rectifying Ca^{2+}-activated

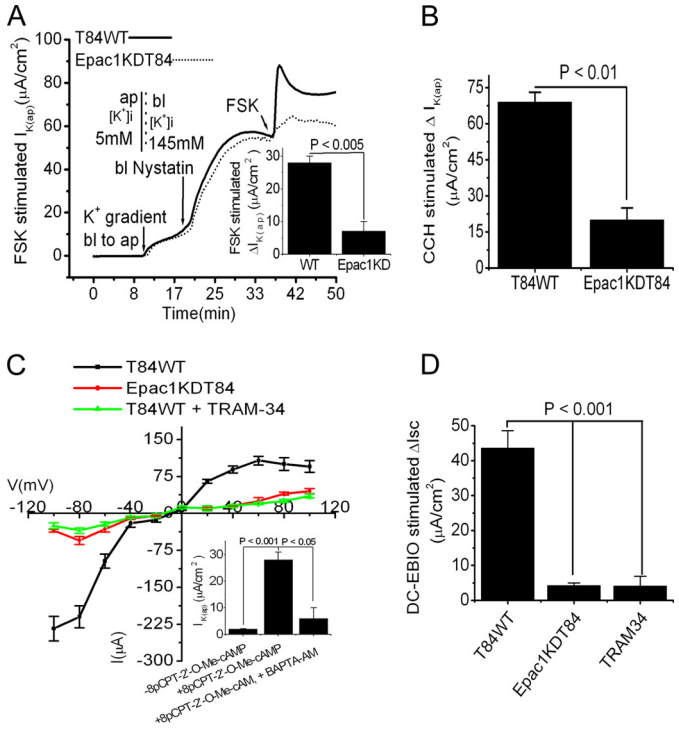

FIGURE 3. **Inhibition of $I_{K(ap)}$ by FSK and CCH and of Isc by DC-EBIO stimulation in Epac1KDT84 cells with basolaterally permeabilized membrane.** *A*, representative $I_{K(ap)}$ recordings in response to FSK (10 μM) in T84WT and Epac1KDT84 cells with imposed basolateral (145 mM) to apical (5 mM) K^+ gradient. The *inset* shows the summary of the data from six such monolayers. Values are mean ± S.E.; $n = 6$. *B*, CCH-stimulated $I_{K(ap)}$ in T84WT and Epac1KDT84 cells. Values are mean ± S.E.; $n = 6$. *C*, I-V relationship in symmetric K^+ concentration in the presence or absence of TRAM-34 in T84WT or Epac1KDT84 cells using the step voltage protocol described under "Materials and Methods." The records are averaged from four independent experiments. The *inset* shows the stimulation of $I_{K(ap)}$ by 8-pCPT-2′-*O*-Me-cAMP in the presence or absence of BAPTA-AM. Values are mean ± S.E.; $n = 4$. *D*, effect of apical DC-EBIO (100 μM) on change in Isc in intact T84WT or Epac1KDT84 cells. T84WT cells were preincubated with or without apical TRAM-34 for 30 min; thereafter, DC-EBIO was added apically. $\Delta I_{K(ap)}$ or Isc was derived from values before and after FSK, CCH, or DC-EBIO stimulation. Values are mean ± S.E.; $n = 6$. *Error bars* represent S.E. *ap*, apical; *bl*, basolateral.

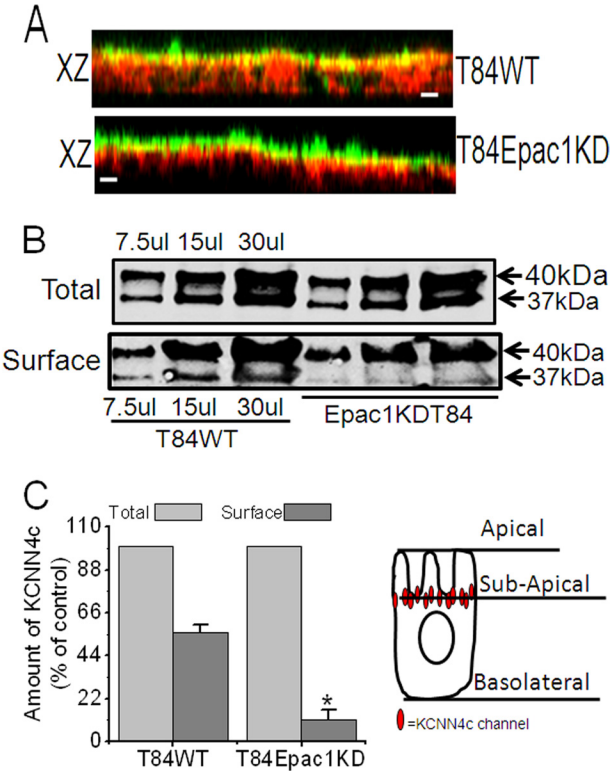

FIGURE 4. **Epac1 depletion affects the KCNN4c protein abundance within the apical plasma membrane of T84WT cells.** *A*, effect of Epac1 depletion on KCNN4c (*red*) colocalization with WGA (*green*) in apical membrane showing loss of colocalization with WGA (*xz* plane; *bottom*) compared with T84WT cells (*xz* plane; *top*). The *scale bar* represents 10 μm. *B*, cell surface expression of KCNN4c (37 kDa) in T84WT and Epac1KDT84 cells as analyzed by the surface biotinylation experiments described under "Materials and Methods." Representative Western blots were quantified with multiple dilutions of total and surface fractions probed with infrared fluorescent IRDye secondary antibody as described under "Materials and Methods." *C*, summary of surface KCNN4c levels (as a percentage of total) of T84WT and Epac1KDT84 cells. The cell illustration demonstrates the mislocalization of KCNN4c immediately beneath the subapical membrane due to depletion of Epac1 (*right*). Experiments were repeated at least three times, and results are shown as mean ± S.E. The *asterisk* (*) indicates a significant difference ($p < 0.05$) from T84WT cells; $n = 3$. *Error bars* represent S.E.

$I_{K(ap)}$ by regulating apical KCNN4c channels in cAMP-stimulated Cl^- secretion.

Epac1 Protein Depletion Resulted in Mislocalization of KCNN4c Channels in T84WT Cells—Because depletion of Epac1 protein unexpectedly caused a significant reduction of $I_{K(ap)}$ even with CCH stimulation, experiments were performed to determine the physical localization of KCNN4c proteins in Epac1KDT84 cells by confocal microscopy. As shown in Fig. 4*A* (*bottom panel*), a reconstructed confocal image in the *xz* plane of Epac1KDT84 monolayers revealed redistribution of KCNN4c proteins into a subapical intracellular compartment detected underneath the apical surface marker WGA. KCNN4c staining overlapped significantly with WGA (Fig. 4*A*, *top panel*), demonstrating that KCNN4c localizes to the apex of T84 epithelia. We speculated that the depletion of Epac1 might lower the surface amount of KCNN4c and thus $I_{K(ap)}$. Therefore, we compared the surface amounts of KCNN4c in T84WT and Epac1KDT84 cells using a biotinylation assay. As shown in Fig. 4, *B* and *C*, Epac1-depleted cells have ~83% lower surface membrane expression of KCNN4c as compared with T84WT cells. The reduced surface amount of the apical version of KCNN4 protein (KCNN4c; 37-kDa band) in the biotinylation assay may explain in part the decrease of $I_{K(ap)}$ in response to both FSK and CCH. These results further support the hypothesis that Epac1 is required for insertion of KCNN4c to the apicalmost cell surface. Additionally, these results are also consistent with FSK stimulation of $I_{K(ap)}$ in Epac1KDT84 cells and with the insignificant effect of 10 μM TRAM-34 (data not shown), although this concentration inhibited the activity of FSK-stimulated Isc and $I_{K(ap)}$ in T84WT cells.

FSK, 8-pCPT-2′-O-Me-cAMP-stimulated Rap1, and Depletion of Rap1A Resulted in Redistribution of KCNN4c into Subapical Region—The role of Epac1-Rap1 signaling in endogenous regulation of KCNN4 was further assessed in T84WT cells by Rap1 activation using Rap1-GTP pulldown assays. We utilized FSK and the novel analog of cAMP, 8-pCPT-2′-*O*-Me-cAMP, a potent activator of the Epac1-Rap1 pathway. 8-pCPT-2′-*O*-Me-cAMP and FSK induced GTP loading of Rap1 in T84WT cells (Fig. 5*A*). To determine whether Rap1, which has two isoforms, Rap1A and Rap1B, is

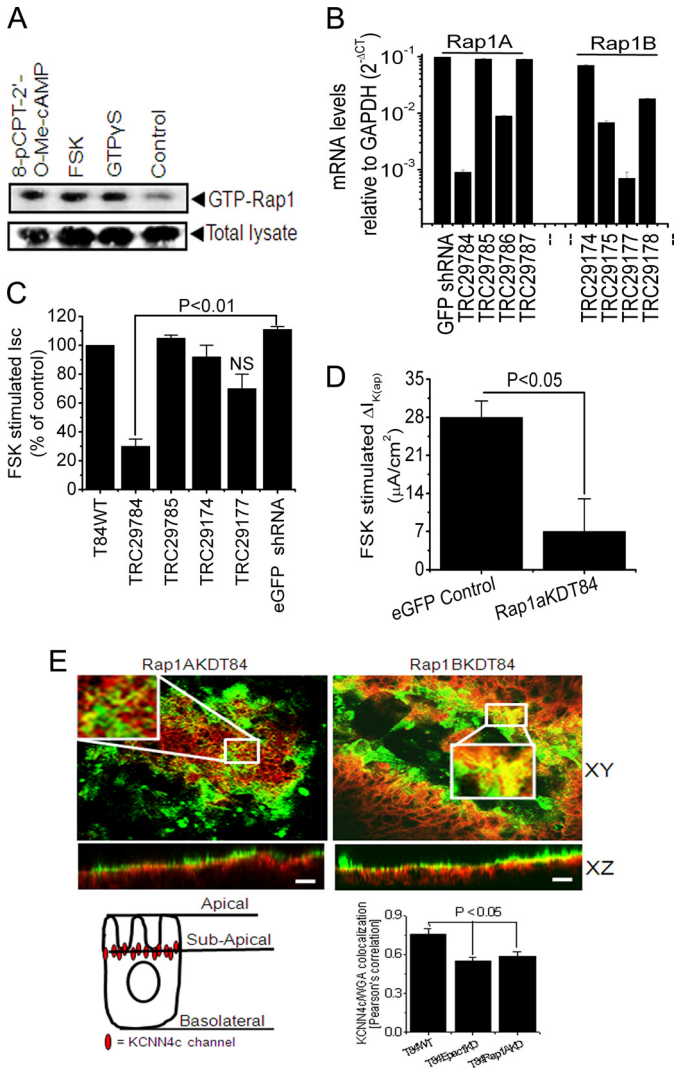

FIGURE 5. **Involvement of Rap1 in FSK-stimulated Isc and $I_{K(ap)}$ through Epac1 stimulation.** *A*, endogenous Rap1 activity was measured with FSK or 8-pCPT-2′-*O*-Me-cAMP or without (control). Cells were incubated in serum-free medium. FSK and 8-pCPT-2′-*O*-Me-cAMP lead to an activation of endogenous Rap1 in T84WT cells. Western blots of total cell lysate probed for total Rap1 are shown as control. Cells loaded with GTPγS and incubated with Ral-GDS-RBD-agarose beads served as a positive control. A representative Western blot of three independent experiments is shown. *B*, quantitative PCR analysis of Rap1A and Rap1B expression in T84WT cells after lenti-shRNA transduction specific for *Rap1A* and *Rap1B* genes, which are shown as mRNA levels relative to levels of GAPDH in log scale. *CT*, cycle threshold. Values are mean ± S.E.; $n = 3$. Summary of the effects of Rap1A and Rap1B knockdown by gene-specific lenti-shRNA on FSK-stimulated Isc (*C*) and $I_{K(ap)}$ (*D*) of Rap1AKDT84 cells. FSK-stimulated Isc in T84WT cells was set to 100% (control). Enhanced GFP (*eGFP*) shRNA-transduced cell monolayers were used as a non-targeting control. Values are mean ± S.E.; $n = 4$. *NS*, statistically not significant. *E*, depletion of Rap1A affected the colocalization of KCNN4c with WGA on the apical membrane as reflected by a significant loss of *yellow* signal in the merged composite (*xy* and *xz* planes; *top left versus top right*). *Insets* show enlarged regions within the *white box*. Confluent Rap1AKDT84 and Rap1BKDT84 cell monolayers were stained with FITC-WGA on ice, then fixed, and stained for KCNN4c (*red*), and a stack of *xz* images was collected by confocal microscopy. A representative *xz* section is shown here. The *scale bar* represents 10 μm. *Bottom right*, quantification of KCNN4c-colocalized WGA in T84WT *versus* Epac1KDT84 or Rap1AKDT84 cells presented as mean ± S.E. by calculating the Pearson's colocalization coefficient using Carl Zeiss LSM software (version 3.2). The cell illustration (*bottom left*) indicates the redistribution of KCNN4c beneath the subapical membrane due to depletion of Epac1 or Rap1A. *Error bars* represent S.E.

involved in the regulation of $I_{K(ap)}$, we used a knockdown approach utilizing lentivirus shRNA in T84WT cells as described previously (27). Quantitative real time PCR was performed on cDNA from RNA preparations of Rap1A and Rap1B knockdown cells, and the mRNA levels were quantified and normalized against GAPDH, which was considered as an endogenous control. We achieved effective knockdown (Fig. 5*b*) with marked reduction of Rap1A and Rap1B transcript levels with constructs TRC29784 and TRC29177, respectively. When Isc or $I_{K(ap)}$ was measured in these knockdown cells grown in a Transwell insert, a significant reduction of Isc or $I_{K(ap)}$ in Rap1AKDT84 cells was observed (Fig. 5, *C* and *D*), whereas depletion of Rap1B alone had no significant effect on FSK-induced Isc (Fig. 5*C*). This observation substantiates the notion that the Epac1-Rap1A signaling pathway may be involved in mobilization of KCNN4c to the cell apical membrane. To test directly the role of Rap1A in the mobilization of KCNN4c to the surface of T84WT cells, confocal microscopy was performed. Confocal images (*xy* and *xz* planes) showed a colocalization of KCNN4c protein and WGA at the apical surface of Rap1BKDT84 cells. On the other hand, colocalization of KCNN4c and WGA was almost absent or found to be low in Rap1AKDT84 cells, whereas KCNN4c localization in the subapical intracellular compartment was increased (Fig. 5*E*, *top panel*). The colocalization signal was quantified by Pearson correlation using Zeiss LSM 510 software. There was a significant reduction of colocalization between KCNN4c and WGA in Rap1AKDT84 cells compared with T84WT or Rap1BKDT84 cells as shown in Fig. 5*E* (*right panel*, *bottom*). These findings suggest that stimulation of $I_{K(ap)}$ required the presence of Rap1A, which might have a role in the redistribution of KCNN4c from the subapical intracellular compartment to the apical plasma membrane.

RhoA, ROCK, and KCNN4 Inhibitors Reduced FSK-stimulated Current and CT-induced Intestinal Fluid Accumulation—Epac1-Rap1 signaling was shown previously to be necessary for translocation of functional α_{2c}-adrenoreceptor to the cell surface involving RhoA and ROCK (41). To better understand the specific involvement of these kinases in KCNN4 regulation in intestinal Cl^- secretion, $I_{K(ap)}$ was measured in T84WT cells. The finding that both RhoA and ROCK kinase inhibitors significantly reduced FSK stimulated $I_{K(ap)}$ (Fig. 6*A*) suggests that cAMP-stimulated $I_{K(ap)}$ conductance requires RhoA and ROCK, which are a downstream target of the Epac1-Rap1 signaling pathway. To determine whether activation of Epac1-Rap1A-RhoA signaling alters the distribution of KCNN4c, cell monolayers were fixed and imaged after stimulation with 8-pCPT-2′-*O*-Me-cAMP either in the presence or absence of ROCK inhibitor H1152. Reconstructed *xz* planes through representative regions are shown in Fig. 6*B*. The apical distribution of KCNN4c is clearly enhanced following 8-pCPT-2′-*O*-Me-cAMP stimulation as evident by the increased colocalization with WGA (Fig. 6*B*, *bottom*), whereas following H1152 treatment, overall colocalization was lower, and KCNN4c congregated immediately below the plasma membrane (Fig. 6*B*, *top*).

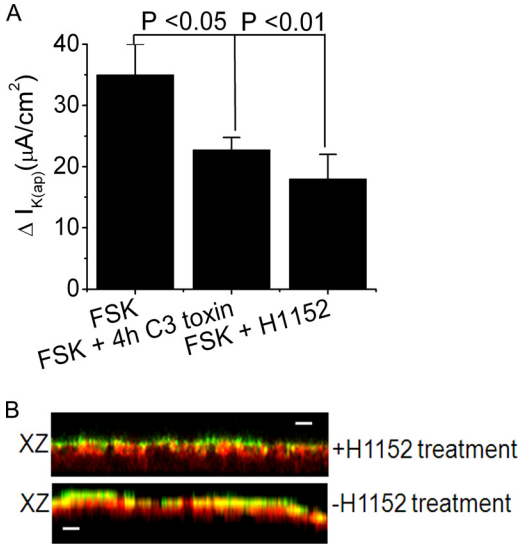

FIGURE 6. **Involvement of Epac1-Rap1A-RhoA-ROCK signaling in intestinal Cl^- secretion.** *A*, summary of the effects of RhoA inhibitor C3 toxin (1 μg/ml) and ROCK inhibitor H1152 (1 μM) on $I_{K(ap)}$. Confluent T84WT cell monolayers on a permeable support were pretreated with C3 toxin for 4 h in culture media prior to subjecting them to the Ussing chamber experiment and with H1152 for 30 min directly in the chamber. FSK was then added. The results are presented as means ± S.E.; $n = 4$. *B*, 8-pCPT-2′-Me-cAMP enhances the insertion of KCNN4c (*red*) into the membrane (*bottom*), and this was partially inhibited by ROCK inhibitor H1152 (*top*). The *scale bar* represents 10 μm. Confluent T84WT cell monolayers were stimulated with 8-pCPT-2′-*O*-Me-cAMP for 30 min at 37 °C prior to staining with FITC-WGA (*green*) on ice, then fixed, and stained for KCNN4c (*red*). *Error bars* represent S.E.

To provide proof of concept that blockade of KCNN4c channels or its regulator, Epac1-Rap1A signaling, could be used in a therapeutic setting, we tested the effect of KCNN4 inhibitor TRAM-34 and Rap1A inhibitor GGTI298 on CT-induced diarrhea in a mouse model (42). In ligated ileal loops, CT treatment stimulated fluid accumulation, which was significantly reduced by TRAM-34 or GGTI298 in a dose-dependent manner (Fig. 7). Additionally, we tested ROCK-mediated inhibition of fluid accumulation in mice that were stimulated by CT. A single dose of ROCK inhibitor H1152 effectively prevented fluid accumulation in the intestinal loop. These results clearly demonstrate that the apical KCNN4c channel requires Rap1A and its downstream signaling targets RhoA and ROCK in CT-induced fluid accumulation.

DISCUSSION

In the present experiments, we demonstrate a novel function for Epac1: the regulation of KCNN4c channels and cAMP-stimulated Cl^- secretion. We hypothesized that the non-CFTR-mediated component of Cl^- secretion stimulated by Epac1 resulted from a cAMP-induced increase of $[Ca^{2+}]_i$ through the Epac1-Rap2-PLC-$[Ca^{2+}]_i$ signaling cascade and required the opening of apical KCNN4c channels to facilitate transepithelial Cl^- secretion by increasing the electrochemical driving force. Our data are consistent with the coupling of apical KCNN4c and non-CFTR Cl^- channels in mediating the Cl^- secretory effect of Epac1. We found that 8-pCPT-2′-*O*-Me-cAMP induced a moderately inwardly rectifying Ca^{2+}-activated $I_{K(ap)}$ response and that the cAMP-stimulated Isc response was inhibited by the KCNN4-specific

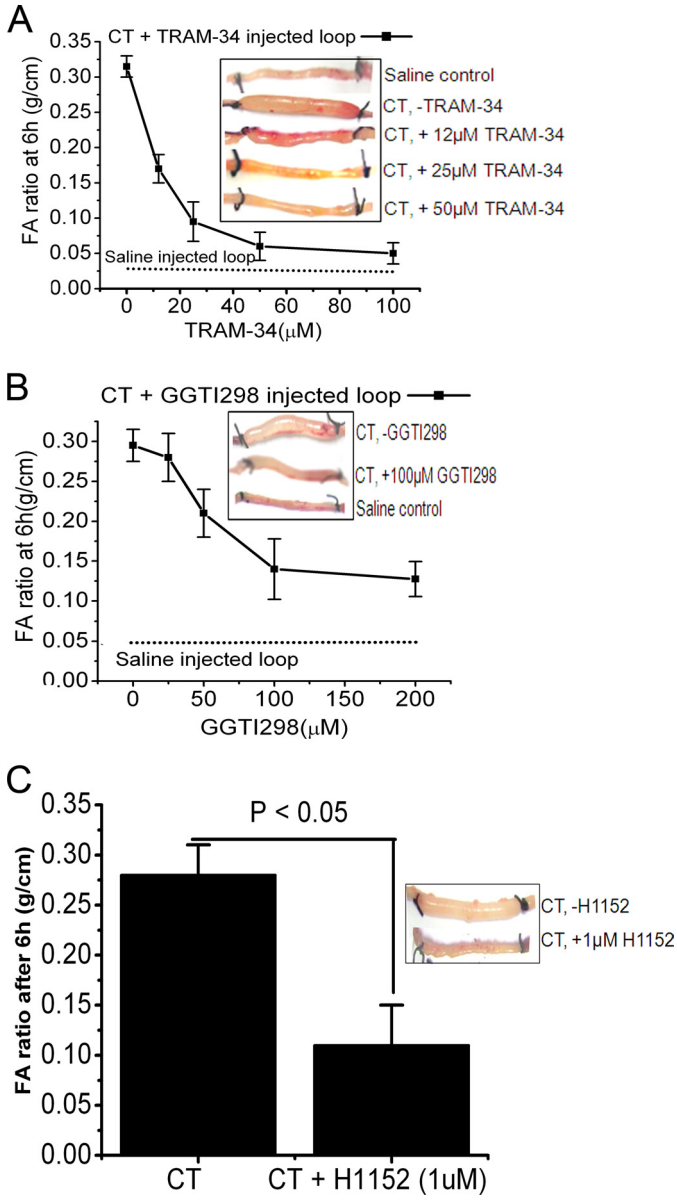

FIGURE 7. **Inhibition of Rap1A, ROCK, or KCNN4c by *in vivo* intestinal loop experiments reduces secretory diarrhea in mice.** Dose-response curves of fluid accumulation (*FA*) ratio in closed mouse ileal loops by CT stimulation in the presence of KCNN4c inhibitor TRAM-34 (*A*) or Rap1A-specific inhibitor GGTI298 (*B*) are shown. A saline control (no CT) is shown for comparison. The *inset* shows a photograph of representative mouse ileal loops at 6 h after luminal injection of CT (1 μg) with or without inhibitors. *C*, a single dose of ROCK inhibitor H1152 (1 μM) inhibits CT-stimulated FA. The bar graph shows the average fluid accumulation ratio at 6 h after CT challenge with or without H1152. The fluid accumulation ratio was calculated as described under "Materials and Methods." Data represent the mean ± S.E.; $n = 10$ mice per group. *Error bars* represent S.E.

inhibitor TRAM-34 in T84WT cells. In contrast to T84WT cells, Epac1KDT84 cells nearly lacked this inwardly rectified $I_{K(ap)}$ current, and the application of TRAM-34 blocked the inwardly rectification in T84WT cells in agreement with the absence of a TRAM-34-sensitive $I_{K(ap)}$. Furthermore, KCNN4c is expressed on the apical membrane of T84WT cells and mouse intestine as shown in Fig. 2*B*. Indeed, much of the KCNN4c colocalized with the plasma membrane marker WGA in T84WT cells, indicating that the primary site of membrane-inserted KCNN4c in these cells is the api-

cal plasma membrane as shown in Fig. 2*A*. Regulation of apical membrane Cl^- channels is often considered to be the primary factor determining the rate of Cl^- secretion (43). Our data show that regulation of apical membrane KCNN4c channels can also determine the rate of Cl^- secretion. This conclusion was best illustrated in Figs. 1*B* and 3*D* where FSK-activated apical KCNN4c (via an increase in $[Ca^{2+}]_i$ by Epac1) resulted in stimulation of apical Cl^- secretion that was ~7 times greater (30 *versus* 4 μA) than in the presence of apical TRAM-34. Similarly, addition of apical DC-EBIO activated apical KCNN4c, stimulating Cl^- secretion that was 10 times greater (44 *versus* 4.1 μA) than in the presence of apical TRAM-34. Thus, the rate of Cl^- secretion can be determined by regulation of either channel (Cl^- or K^+) at the apical membrane. Recently, we have shown that Epac1 in response to cAMP stimulates intestinal Cl^- secretion through a Cl^- channel other than CFTR in a Rap2-PLCϵ-$[Ca^{2+}]_i$-dependent manner (27). However, activation of Rap1 by cAMP is also achieved by the binding of cAMP to Epac proteins, which function as G protein exchange factors for Rap1 (44–46). The role of Rap1 in intestinal epithelial ion transport remains relatively unexplored.

We were also interested in determining the role of KCNN4c channels in cAMP- and/or Epac1-stimulated Cl^- secretion. It appears that KCNN4c is required for cAMP-stimulated Epac1-dependent Cl^- secretion. First, FSK-stimulated Isc was significantly abolished by apical application of the KCNN4 specific inhibitor TRAM-34 but not by BK or SK channel inhibitors. It has been demonstrated before that BK channels are not involved in stimulated electrogenic Cl^- secretion, which is consistent with our present finding (24). Second, KCNN4c channel opener DC-EBIO failed to increase Isc or FSK-stimulated $I_{K(ap)}$ in Epac1-depleted cells. This notion was further supported by our previous study showing that only the cAMP-stimulated Epac1-dependent Cl^- conductance (I_{Cl}) and Isc were abolished in Epac1-depleted cells without any effect on PKA-dependent CFTR-mediated I_{Cl} (27). It is unlikely that the effect of Epac1 depletion caused the reduction of calcium-activated chloride channel protein expression that resulted in complete abolition of I_{Cl} because the calcium agonist CCH-stimulated I_{Cl} was essentially unaffected (only a moderate reduction was observed; data not shown). In contrast to the increasing confusion surrounding the role of a non-CFTR channel in Epac1-stimulated Cl^- secretion, a role for calcium-activated chloride channel has progressed. This of course does not exclude the possibility that Epac1 and its downstream signaling may activate Ca^{2+}-dependent apical KCNN4c channels, hyperpolarize the cells, and result in Cl^- secretion.

These observations support the interpretation that there is a coupling between KCNN4c and Epac1-stimulated Cl^- secretion. However, our results further demonstrated a novel effect of Rap1 in intestinal epithelial cells: the stimulation of KCNN4c is apparently caused by the activation of a Rap1-dependent pathway, which is dependent on Epac1 and leads to a RhoA-ROCK-mediated rapid incorporation of functional KCNN4c into the apical surface. Several lines of evidence support this hypothesis. First, depletion of Epac1 decreased KCNN4c protein abundance at the cell surface but not that of KCNN4b protein as shown by the surface biotinylation study (Fig. 4*B*). Second, CCH, FSK, or 8-pCPT-2′-*O*-Me-cAMP and DC-EBIO failed to stimulate the $I_{K(ap)}$, Isc, or inwardly rectifying Ca^{2+}-activated K^+ current in Epac1KDT84 cells with the reduction of Cl^- secretion by CCH stimulation in Epac1KDT84 cells clearly explaining the loss of functional KCNN4c in the apical surface. Third, FSK and the Epac activator 8-pCPT-2′-*O*-Me-cAMP both increased active Rap1 (GTP-Rap1) in T84WT cells. Fourth, H1152, a ROCK inhibitor, significantly reduced cAMP-stimulated $I_{K(ap)}$ in T84WT cells. In most cell types, RhoA acts as an upstream signaling molecule to activate ROCK, which in turn is involved in the translocation of protein to the cell surface (47, 48). A similar signaling module has been described in microvascular smooth muscle cells (49). In line with previously described ROCK functional data, we observed a significant reduction in colocalization of KCNN4c with WGA in T84WT cells pretreated with ROCK inhibitor, whereas 8-pCPT-2′-*O*-Me-cAMP induced this colocalization to the apical surface in the absence of this inhibitor. The findings described above demonstrate for the first time rapid KCNN4c mobility in T84 epithelia as a dynamic process that is regulated by Epac1 stimulation with a time scale of 30 min that involves ROCK and remain to be investigated. We found that the colocalization of KCNN4c and WGA markedly increased in T84WT cells in contrast to the marked decrease in Epac1KDT84 cells. This is consistent with our observations that the surface amount of KCNN4c was significantly reduced in Epac1KDT84 cells, whereas KCNN4b levels in the basolateral membrane were unaffected (Fig. 4*B*). The decreased amount of surface KCNN4c and increased amount of KCNN4c in the subapical compartment in Epac1KDT84 cells are in good agreement with a predominate role of apical KCNN4c in mediating the effect of Epac1 in Cl^- secretion. These observations indicate that Epac1 may play a critical role in the distribution of KCNN4c and its activation via the Rap1A-RhoA-ROCK signaling pathway. Epac1-Rap1 signaling could enhance the protein abundance in the cell membrane either by insertion of KCNN4c in the apical surface or by delaying the retrieval of this channel protein from the membrane. It is not readily evident at present which of these two possibilities is correct; future experiments will be required. Finally, to explore the therapeutic potential of KCNN4c channel blockade in the regulation of active Cl^- secretion and its regulation by Epac1 signaling, we tested the effect of the Rap1A inhibitor GGTI298, the ROCK inhibitor H1152, and the KCNN4c inhibitor TRAM-34 in a closed loop mouse model. A significant decrease in intestinal fluid accumulation was observed in mice that received any one of these compounds. These results clearly demonstrated that inhibiting Epac1-Rap1-RhoA-ROCK signaling may represent a novel, potential therapeutic approach for the treatment of diarrhea that is mediated by cAMP by interfering with the recruitment of KCNN4c to the apical membrane.

In conclusion, we have demonstrated for the first time that apical KCNN4c channel expression and activity are markedly decreased due to Epac1 depletion involving Rap1A-RhoA-ROCK signaling and provide a molecular framework for new understanding of the regulation of epithelial Cl^- secretion. More importantly, the identification of TRAM-34 and its effec-

tive antisecretory role in both cultured cell monolayers and *in vivo* in mice represents a promising new platform upon which a new therapy for diarrhea and other gastrointestinal disorders could be developed.

Acknowledgments—We gratefully acknowledge the help and research facilities provided by Dr. Shekhar Chakraborty, Director, National Institute of Cholera and Enteric Diseases, Kolkata, India. We also acknowledge the Gastroenterology Division of The Johns Hopkins University for the use of research facilities for this study.

REFERENCES

1. Dubyak, G. R. (2004) Ion homeostasis, channels, and transporters: an update on cellular mechanisms. *Adv. Physiol. Educ.* **28,** 143–154
2. Barrett, K. E. (2008) New ways of thinking about (and teaching about) intestinal epithelial function. *Adv. Physiol. Educ.* **32,** 25–34
3. Kiela, P. R., and Ghishan, F. K. (2009) Ion transport in the intestine. *Curr. Opin. Gastroenterol.* **25,** 87–91
4. Venkatasubramanian, J., Ao, M., and Rao, M. C. (2010) Ion transport in the small intestine. *Curr. Opin. Gastroenterol.* **26,** 123–128
5. Petri, W. A., Jr., Miller, M., Binder, H. J., Levine, M. M., Dillingham, R., and Guerrant, R. L. (2008) Enteric infections, diarrhea, and their impact on function and development. *J. Clin. Investig.* **118,** 1277–1290
6. Field, M. (2003) Intestinal ion transport and the pathophysiology of diarrhea. *J. Clin. Investig.* **111,** 931–943
7. Geibel, J. P. (2005) Secretion and absorption by colonic crypts. *Annu. Rev. Physiol.* **67,** 471–490
8. Kunzelmann, K., and Mall, M. (2002) Electrolyte transport in the mammalian colon: mechanisms and implications for disease. *Physiol. Rev.* **82,** 245–289
9. Barrett, K. E., and Keely, S. J. (2000) Chloride secretion by the intestinal epithelium: molecular basis and regulatory aspects. *Annu. Rev. Physiol.* **62,** 535–572
10. Keely, S. J., and Barrett, K. E. (2000) Regulation of chloride secretion. Novel pathways and messengers. *Ann. N.Y. Acad. Sci.* **915,** 67–76
11. Warth, R., and Barhanin, J. (2003) Function of K^+ channels in the intestinal epithelium. *J. Membr. Biol.* **193,** 67–78
12. Hamilton, K. L., and Devor, D. C. (2012) Basolateral membrane K channels in renal epithelial cells. *Am. J. Physiol. Renal Physiol.* **302,** F1069–F1081
13. Turnheim, K., Plass, H., and Wyskovsky, W. (2002) Basolateral potassium channels of rabbit colon epithelium: role in sodium absorption and chloride secretion. *Biochim. Biophys. Acta* **1560,** 51–66
14. Almassy, J., Won, J. H., Begenisich, T. B., and Yule, D. I. (2012) Apical Ca^{2+}-activated potassium channels in mouse parotid acinar cells. *J. Gen. Physiol.* **139,** 121–133
15. Palmer, M. L., Schiller, K. R., O'Grady, S. M. (2008) Apical SK potassium channels and Ca^{2+}-dependent anion secretion in endometrial epithelial cells. *J. Physiol.* **586,** 717–726
16. Greger, R., Bleich, M., Riedemann, N., van Driessche, W., Ecke, D., and Warth, R. (1997) The role of K^+ channels in colonic Cl^- secretion. *Comp. Biochem. Physiol. A Physiol.* **118,** 271–275
17. Cook, D. I., and Young, J. A. (1989) Effect of K^+ channels in the apical plasma membrane on epithelial secretion based on secondary active Cl^- transport. *J. Membr. Biol.* **110,** 139–146
18. Nanda Kumar, N. S, Singh, S. K., and Rajendran, V. M. (2010) Mucosal potassium efflux mediated via Kcnn4 channels provides the driving force for electrogenic anion secretion in colon. *Am. J. Physiol. Gastrointest. Liver Physiol.* **299,** G707–G714
19. Warth, R., Hamm, K., Bleich, M., Kunzelmann, K., von Hahn, T., Schreiber, R., Ullrich, E., Mengel, M., Trautmann, N., Kindle, P., Schwab, A., and Greger, R. (1999) Molecular and functional characterization of the small Ca^{2+}-regulated K^+ channel (rSK4) of colonic crypts. *Pflugers Arch.* **438,** 437–444
20. Wulff, H., Kolski-Andreaco, A., Sankaranarayanan, A., Sabatier, J. M., and Shakkottai, V. (2007) Modulators of small- and intermediate-conductance calcium-activated potassium channels and their therapeutic indications. *Curr. Med. Chem.* **14,** 1437–1457
21. Begenisich, T., Nakamoto, T., Ovitt, C. E., Nehrke, K., Brugnara, C., Alper, S. L., and Melvin, J. E. (2004) Physiological roles of the intermediate conductance, Ca^{2+}-activated potassium channel Kcnn4. *J. Biol. Chem.* **279,** 47681–47687
22. Barmeyer, C., Rahner, C., Yang, Y., Sigworth, F. J., Binder, H. J., and Rajendran, V. M. (2010) Cloning and identification of tissue specific expression of kcnn4 splice variants in rat colon. *Am. J. Physiol. Cell Physiol.* **299,** C251–C263
23. Reinhart, P. H., Chung, S., Martin, B. L., Brautigan, D. L., and Levitan, I. B. (1991) Modulation of calcium-activated potassium channels from rat brain by protein kinase A and phosphatase 2A. *J. Neurosci.* **11,** 1627–1635
24. Matos, J. E., Sausbier, M., Beranek, G., Sausbier, U., Ruth, P., and Leipziger, J. (2007) Role of cholinergic-activated KCa1.1 (BK), KCa3.1 (SK4) and KV7.1 (KCNQ1) channels in mouse colonic Cl^- secretion. *Acta Physiol.* **189,** 251–258
25. Gerlach, A. C., Gangopadhyay, N. N., and Devor, D. C. (2000) Kinase-dependent regulation of the intermediate conductance, calcium-dependent potassium channel, hIK1. *J. Biol. Chem.* **275,** 585–598
26. Gerlach, A. C., Syme, C. A., Giltinan, L., Adelman, J. P., and Devor, D. C. (2001) ATP-dependent activation of the intermediate conductance, Ca^{2+}-activated K^+ channel, hIK1, is conferred by a C-terminal domain. *J. Biol. Chem.* **276,** 10963–10970
27. Hoque, K. M., Woodward, O. M., van Rossum, D. B., Zachos, N. C., Chen, L., Leung, G. P., Guggino, W. B., Guggino, S. E., and Tse, C. M. (2010) Epac1 mediates protein kinase A-independent mechanism of forskolin-activated intestinal chloride secretion. *J. Gen. Physiol.* **135,** 43–58
28. Mun, E. C., Mayol, J. M., Riegler, M., O'Brien, T. C., Farokhzad, O. C., Song, J. C., Pothoulakis, C., Hrnjez, B. J., and Matthews, J. B. (1998) Levamisole inhibits intestinal Cl^- secretion via basolateral K^+ channel blockade. *Gastroenterology* **114,** 1257–1267
29. Broere, N., Hillesheim, J., Tuo, B., Jorna, H., Houtsmuller, A. B., Shenolikar, S., Weinman, E. J., Donowitz, M., Seidler, U., de Jonge, H. R., and Hogema, B. M. (2007) Cystic fibrosis transmembrane conductance regulator activation is reduced in the small intestine of Na^+/H^+ exchanger 3 regulatory factor 1 (NHERF-1)- but not NHERF-2-deficient mice. *J. Biol. Chem.* **282,** 37575–37584
30. Strohmeier, G. R., Lencer, W. I., Patapoff, T.W., Thompson, L. F., Carlson, S. L., Moe, S. J., Carnes, D. K., Mrsny, R. J., and Madara, J. L. (1997) Surface expression, polarization, and functional significance of CD73 in human intestinal epithelia. *J. Clin. Investig.* **99,** 2588–2601
31. Sarker, R., Grønborg, M., Cha, B., Mohan, S., Chen, Y., Pandey, A., Litchfield, D., Donowitz, M., and Li, X. (2008) Casein kinase 2 binds to the C terminus of Na^+/H^+ exchanger 3 (NHE3) and stimulates NHE3 basal activity by phosphorylating a separate site in NHE3. *Mol. Biol. Cell* **19,** 3859–3870
32. Murtazina, R., Kovbasnjuk, O., Chen, T. E., Zachos, N. C., Chen, Y., Kocinsky, H. S., Hogema, B. M., Seidler, U., de Jonge, H. R., and Donowitz, M. (2011) NHERF2 is necessary for basal activity, second messenger inhibition, and LPA stimulation of NHE3 in mouse distal ileum. *Am. J. Physiol. Cell Physiol.* **301,** C126–C136
33. Devys, D., Lutz, Y., Rouyer, N., Bellocq, J. P., and Mandel, J. L. (1993) The FMR-1 protein is cytoplasmic, most abundant in neurons and appears normal in carriers of a fragile X premutation. *Nat. Genet.* **4,** 335–340
34. De, S. N., and Chatterje, D. N. (1953) An experimental study of the mechanism of action of Vibrio cholerae on the intestinal mucous membrane. *J. Pathol. Bacteriol.* **66,** 559–562
35. Barrett, K. E. (1993) Positive and negative regulation of chloride secretion in T84WT cells. *Am. J. Physiol. Cell Physiol.* **265,** C859–C868
36. Rufo, P. A., Jiang, L., Moe, S. J., Brugnara, C., Alper, S. L., and Lencer, W. I. (1996) The antifungal antibiotic, clotrimazole, inhibits Cl^- secretion by polarized monolayers of human colonic epithelial cells. *J. Clin. Investig.* **98,** 2066–2075
37. Rufo, P. A., Merlin, D., Riegler, M., Ferguson-Maltzman, M. H., Dickinson, B. L., Brugnara, C., Alper, S. L., and Lencer, W. I. (1997) The antifungal antibiotic, clotrimazole, inhibits chloride secretion by human intestinal

T84WT cells via blockade of distinct basolateral K^+ conductances. Demonstration of efficacy in intact rabbit colon and in an *in vivo* mouse model of cholera. *J. Clin. Investig.* **100,** 3111–3120
38. Duffey, M. E., Mongiardo, K., Hallman, J., and Crane, J. K. (2012) Zn^{2+} has biphasic effects on KCNQ1/KCNE3 K^+ channels. *FASEB J.* **26,** 1152.9
39. Chan, H. C., Cheung, W. T., Leung, P. Y., Wu, L. J., Chew, S. B., Ko, W. H., and Wong, P. Y. (1996) Purinergic regulation of anion secretion by cystic fibrosis pancreatic duct cells. *Am. J. Physiol. Cell Physiol.* **271,** C469–C477
40. Singh, S. K., O'Hara, B., Talukder, J. R., and Rajendran, V. M. (2012) Aldosterone induces active K^+ secretion by enhancing mucosal expression of Kcnn4c and Kcnma1 channels in rat distal colon. *Am. J. Physiol. Cell Physiol.* **302,** C1353–C1360
41. Jeyaraj, S. C., Unger, N. T., Eid, A. H., Mitra, S., Paul El-Dahdah, N., Quilliam, L. A., Flavahan, N. A., and Chotani, M. A. (2012) Cyclic AMP-Rap1A signaling activates RhoA to induce α_{2c}-adrenoceptor translocation to the cell surface of microvascular smooth muscle cells. *Am. J. Physiol. Cell Physiol.* **303,** C499–C511
42. Ma, T., Thiagarajah, J. R., Yang, H., Sonawane, N. D., Folli, C., Galietta, L. J., and Verkman, A. S. (2002) Thiazolidinone CFTR inhibitor identified by high-throughput screening blocks cholera toxin-induced intestinal fluid secretion. *J. Clin. Investig.* **110,** 1651–1658
43. Welsh, M. J. (1987) Electrolyte transport by airway epithelia. *Physiol. Rev.* **67,** 1143–1184
44. Caron, E. (2003) Cellular functions of the Rap1 GTP-binding protein: a pattern emerges. *J. Cell Sci.* **116,** 435–440
45. Wang, Z., Dillon, T. J., Pokala, V., Mishra, S., Labudda, K., Hunter, B., and Stork, P. J. (2006) Rap1-mediated activation of extracellular signal-regulated kinases by cyclic AMP is dependent on the mode of Rap1 activation. *Mol. Cell. Biol.* **26,** 2130–2145
46. Pochynyuk, O., Stockand, J. D., and Staruschenko, A. (2007) Ion channel regulation by Ras, Rho, and Rab small GTPases. *Exp. Biol. Med.* **232,** 1258–1265
47. Pochynyuk, O., Medina, J., Gamper, N., Genth, H., Stockand, J. D., and Staruschenko, A. (2006) Rapid translocation and insertion of the epithelial Na^+ channel in response to RhoA signaling. *J. Biol. Chem.* **281,** 26520–26527
48. Bezzerides, V. J., Ramsey, I. S., Kotecha, S., Greka, A., and Clapham, D. E. (2004) Rapid vesicular translocation and insertion of TRP channels. *Nat. Cell Biol.* **6,** 709–720
49. Eid, A. H., Chotani, M. A., Mitra, S., Miller, T. J., and Flavahan, N. A. (2008) Cyclic AMP acts through Rap1 and JNK signaling to increase expression of cutaneous smooth muscle α_{2C}-adrenoceptors. *Am. J. Physiol. Heart Circ. Physiol.* **295,** H266–H272